

# Mesoporous Carbon Membranes from Polyimide Blended with Poly(ethylene glycol)

H. HATORI,<sup>1</sup> T. KOBAYASHI,<sup>1</sup> Y. HANZAWA,<sup>1</sup> Y. YAMADA,<sup>1</sup> Y. IIMURA,<sup>2</sup> T. KIMURA,<sup>2</sup> M. SHIRAISHI<sup>3</sup>

<sup>1</sup>National Institute for Resources and Environment, 16-3 Onogawa, Tsukuba 305-8569, Japan

<sup>2</sup>Shibaura Institute of Technology, 9-14 Shibaura 3-chome Minato-ku, Tokyo 108-0023, Japan

<sup>3</sup>Tokai University, 317 Nishino, Numazu, Shizuoka 410-0395, Japan

Received 7 January 2000; accepted 8 March 2000

**ABSTRACT:** The control of the mesoporous structure in a carbon membrane from a poly(ethylene glycol)/polyimide-blended polymer was investigated. The size of the pores tends to become large with increase of the content of poly(ethylene glycol) against polyimide, that is, the mesoporous structure could be controlled by the composition of the blended polymers. On the other hand, the average molecular weight of poly(ethylene glycol) has little effect from the viewpoint of the control of the pore structure. © 2000 John Wiley & Sons, Inc. *J Appl Polym Sci* 79: 836–841, 2001

**Key words:** mesoporous carbon membrane; polymer blend; polyimide-based carbon; poly(ethylene glycol)

## INTRODUCTION

Activated carbon, a representative porous carbon material, is used in a wide variety of applications such as in water or gas purification, decolorizing, solvent recovery, and protective filters.<sup>1</sup> Recently, porous carbon material was also applied to methane storage adsorbents<sup>2,3</sup> or electrodes of an electric double-layer capacitor.<sup>4</sup> Conventional activated carbon has a wide range of pore sizes classified by IUPAC into three categories according to their size: micropore (<2 nm), mesopore (2–50 nm), and macropore (>50 nm).<sup>5</sup> In recent applications as electrodes or adsorbents for energy storage, however, porous carbon material is evaluated not only in unit per weight but also in unit

per volume. Therefore, the pores that are effective in these applications must be condensed and other pores, which decrease the adsorbence per volume because of the decrease of the packing density, must be excluded. This indicates the importance of the methods which can control the pore structure in a wide of nanometer-to-micrometer range.

We have already reported on various types of porous carbon films prepared from polyimide; non-porous polyimide film gave microporous carbon with molecular sieving properties<sup>6,7</sup> and macroporous carbon was prepared from the phase-inversion membrane.<sup>8</sup> In our preliminary work,<sup>9,10</sup> we found that polyimide blended with some kinds of polymers is a good precursor of porous carbon. For example, poly(4,4'-oxydiphenylene pyromellitimide) blended with poly(methyl methacrylate) gave a macroporous film, while poly(*para*/phenylene pyromellitimide) with poly(ethylene glycol) yielded a mesoporous carbon film. There are some methods which can prepare mesoporous carbon.<sup>11–13</sup> How-

Correspondence to: H. Hatori.

Contract grant sponsor: Japan Society for the Promotion of Science; contract grant number: JSPS-RFTF96R11701.

*Journal of Applied Polymer Science*, Vol. 79, 836–841 (2001)  
© 2000 John Wiley & Sons, Inc.

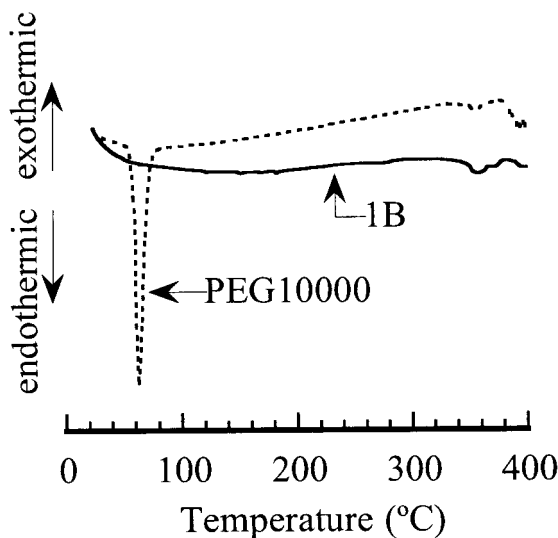


**Figure 1** DTA curves of PEG10,000 and 1B (PEG-10,000/PI = 0.85/1).

ever, preparation of porous carbon from a polymer blend is achieved by a much simpler procedure than by the other methods: by just blending and carbonization. In addition, special application is expected by the membrane form, just as the microporous carbon showed a high performance as a gas-separation membrane.<sup>6,14–17</sup> In the present article, we investigated how to control the mesoporous structure in a carbon membrane from a poly(*para*/phenylene pyromellitimide)/poly(ethylene glycol)-blended polymer.

## EXPERIMENTAL

### Samples

A solution of poly(*para*/phenylene pyromellitic acid) (PAA, 10 g) in 40 mL of *N,N*-dimethylacetamide (DMAc) was prepared from pyromellitic dianhydride and *para*/phenylenediamine by the method of Dine-Hart and Wright.<sup>18</sup> A solution of poly(ethylene glycol) (PEG) in 30 mL of DMAc was added and stirred for 3 h. Commercially available PEG (Wako Pure Chemical Industries, Ltd., Japan) was used without further purification and was represented by “PEG” plus “the average molecular weight” ( $M_n$ ), such as PEG2000. The mixed solution was cast onto a glass substrate and evacuated at 60°C. After removal from the substrate, the films were treated at 200°C for 3 h in order to change PAA into polyimide (PI).

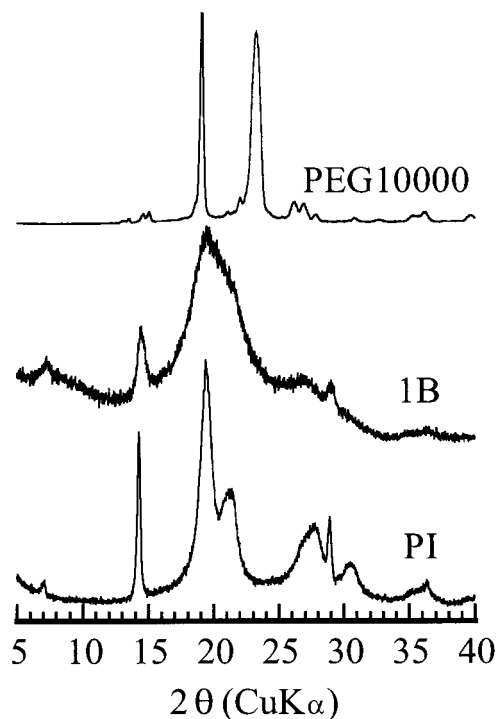


**Figure 2** X-ray diffraction profiles of PEG10,000, 1B (PEG10,000/PI = 0.85/1), and PI.

Translucent films were prepared when PEG-2000, PEG10,000 or PEG20,000 was blended with the weight ratio of PEG/PI = 0.85/1. The ratio was the maximum limit of PEG10,000 without the separation of PEG out of the film. It was impossible to have a blended film from PEG100,000 because the clear solution in DMAc was not given when mixed with PAA at

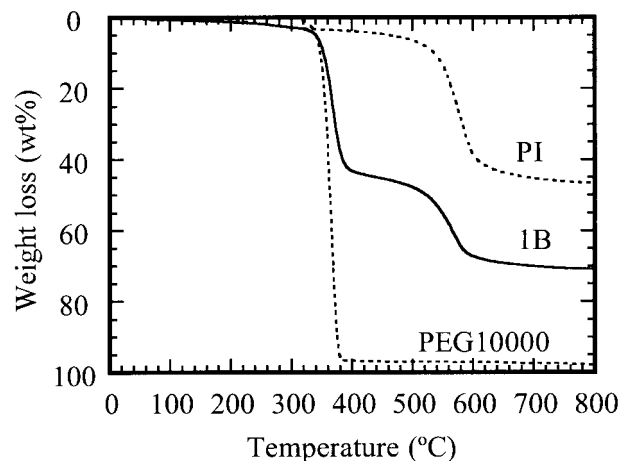


**Figure 3** TGA curves of PEG10,000, 1B (PEG-10,000/PI = 0.85/1), and PI.

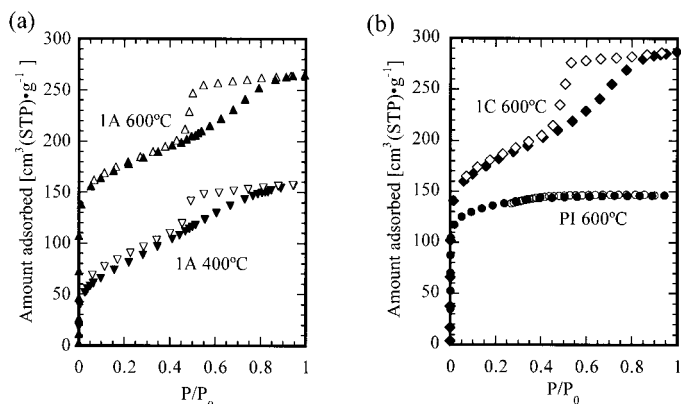


**Figure 4** Nitrogen-adsorption isotherms at 77K: (a) 1A (PEG2000/PI = 0.85/1) treated at 400 and 600°C; (b) 1C (PEG20,000/PI = 0.85/1) and PI treated at 600°C; closed symbols: adsorption, open symbols: desorption.

the same ratio. The blended films at a 0.85/1 ratio are abbreviated 1A, 1B, and 1C for the samples using PEGs with an  $M_n$  of 2000, 10,000, and 20,000, respectively. PEG2000-blended films with various ratios larger than 0.85/1 were prepared as well. The samples were shown by a factor against the 0.85/1 ratio, for example, the PEG/PI = 1.7/1 sample is abbreviated as 2A. Films were translucent or opaque when the ratio was less than that of 2A. The 4A and 8A samples were flakes, because the samples could not be removed from the glass substrate as thin films. The samples were heat-treated at a heating rate of 3 K/min in flowing argon and carbonized at 600°C for 1 h.

### Analysis

Thermogravimetric analysis (TGA) and differential thermal analysis (DTA) were done using a TAS 200 system (RIGAKU Co., Ltd.). Nitrogen-adsorption isotherms were measured at 77 K using a Belsorp 28SA (BEL Japan, Inc.). The Cranston–Inkley method<sup>19</sup> was used to determine the mesopore volume ( $V_{\text{meso}}$ ) and the pore-size distribution in the range of the mesopore. The micropore volume ( $V_{\text{micro}}$ ) was calculated from the difference between the mesopore volume and the adsorption capacity ( $V_{\text{cap}}$ ) determined from the liquid volume of nitrogen taken up at an alternative pressure of  $p/p_0 = 0.95$ . A mercury porosimeter (Pore Master33, QuantaChrome) was used for measurement of the macropore volume ( $V_{\text{macro}}$ ) and the pore-size distribution at the larger size.

## RESULTS AND DISCUSSION

### Structural Change in Carbonization and the Dependence on $M_n$

DTA curves of PEG10,000 and 1B are shown in Figure 1. Despite the sharp peak on the curve of PEG10,000 at the melting point, no peak was observed on that of 1B. The result shows the quite high compatibility between PI and PEG in 1B film. On the other hand, the peaks of a PI crystallite were observed in an X-ray profile of 1B (Fig. 2), indicating the presence of PI domains. From these results, microphase separation in 1B film is predictable.

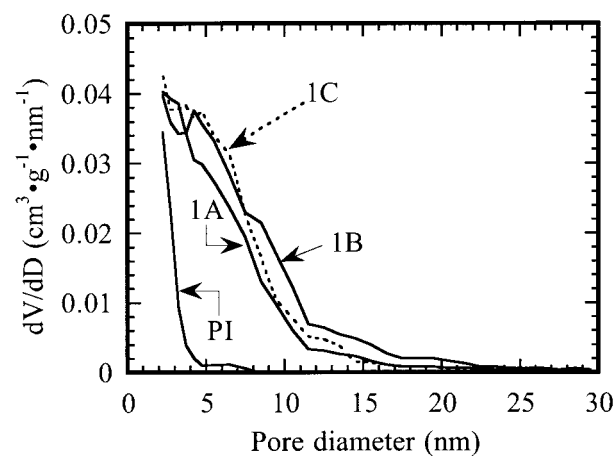


**Figure 5** Pore-size distribution curves of carbonized samples from PI blended with PEGs having different  $M_n$ : 1A (PEG2000/PI = 0.85/1), 1B (PEG10,000/PI = 0.85/1), and 1C (PEG20,000/PI = 0.85/1).

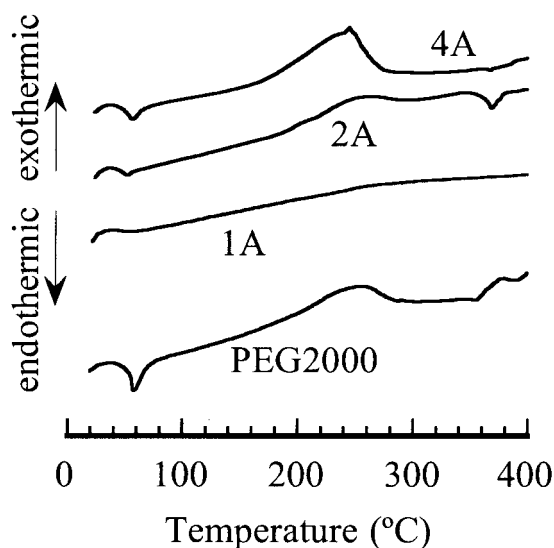


**Figure 6** DTA curves of PEG2000 and the blended films: 1A (PEG2000/PI = 0.85/1), 2A (PEG2000/PI = 1.7/1), and 4A (PEG2000/PI = 3.4/1).

The representative result of TGA is shown in Figure 3. No carbon residue is yielded from PEG with any  $M_n$  by the treatment above 400°C, as decomposed to volatile matters. The curve of 1B shows that PEG decomposes as a first step, followed by the polyimide pyrolysis. The curve corresponding well to that predicted from those of homopolymers, PI and PEG10,000, indicates that each polymer is individually carbonized in 1B film without coprolysis.

Nitrogen-adsorption isotherms of samples treated at 400 and 600°C are shown in Figure 4. The blended films after carbonization at 600°C gave the isotherms having hysteresis, which appears when the sample has a mesoporous struc-

ture.<sup>20</sup> The isotherms indicate that the carbonized samples given from the blended films have a considerable amount of mesopores in addition to micropores, while the PI homopolymer carbonized at 600°C has a microporous structure without mesopores [Fig. 4(b)], similarly to the molecular-sieving carbon films obtained from Kapton-type polyimide.<sup>7</sup>

It is shown from the isotherm of 1A treated at 400°C [Fig. 4(a)] that the mesopore was generated at 400°C before carbonization of PI, although the sample is less microporous. Such a mesoporous polymer membrane is interesting as well, but the pore structure and the properties should be investigated by the other methods suited for the analysis of the polymer material. In any event, microphase separation at a polymer stage and the formation of a mesoporous structure by the decomposition of PEG suggest that the mesopores are originated from the PEG domains which are decomposed to volatile matters by heat treatment.

Pore-size distribution curves determined from the nitrogen-adsorption isotherm using the Cranston–Inkley method are shown in Figure 5. There are some differences of the mesopore volume, which is 0.222, 0.308, and 0.261 cm<sup>3</sup>/g for carbonized 1A, 1B and 1C, respectively. However, the pore-size distribution curves of these samples are not appreciably different. The influence of the PEG  $M_n$  is fundamentally not enough from the viewpoint of the control of the pore structure.

#### Change of the Pore-size Distribution by PEG/PI Composition

The endothermic peak at the melting point (60°C) was not detected on the DTA curve of 1A (Fig. 6)

**Table I** Carbonization Yield of PEG2000-blended Samples and the Pore Volumes in Each Size

Pristine Sample	Carbon Yield <sup>a</sup> (wt %)	$V_{\text{cap}}$ <sup>b</sup> (cm <sup>3</sup> /g)	$V_{\text{micro}}$ <sup>b</sup> (cm <sup>3</sup> /g)	$V_{\text{meso}}$ (cm <sup>3</sup> /g)	$V_{\text{macro}}$ <sup>c</sup> (cm <sup>3</sup> /g)
PI	61.3	0.232	0.191	0.041	—
1/2A	43.8 (43.0)	0.313	0.202	0.111	0.01
1A	32.3 (33.1)	0.417	0.195	0.222	<0.01
3/2A	27.5 (27.0)	0.446	0.193	0.253	<0.01
2A	22.6 (22.7)	0.506	0.187	0.319	<0.01
4A	14.5 (13.9)	0.535	0.196	0.339	0.13
8A	8.7 (7.9)	0.534	0.189	0.345	0.85

<sup>a</sup> Carbon yields at 600°C and theoretical yields in the parentheses.

<sup>b</sup> Micropore volumes calculated by  $V_{\text{micro}} = V_{\text{cap}} - V_{\text{meso}}$ .

<sup>c</sup> Macropore volumes (50–1000 nm) determined by mercury porosimetry.

as it was for 1B (Fig. 1). On the other hand, the peak was barely observed for 2A and became clear for the sample with higher PEG contents (Fig. 6). The result suggests a larger domain size of PEG at higher PEG/PI ratios.

Carbonization yields of PEG2000-blended films are listed in Table I with the theoretical yields, which were calculated on the basis of the hypotheses of (1) no change of PI carbon yield by PEG pyrolysis and (2) no carbon residue from PEG. The correspondence between the experimental value and the theoretical one indicates the validity of the hypotheses in each sample.

Changes in the pore-size distribution curves are shown in Figures 7 and 8, which were determined by a nitrogen-adsorption measurement and mercury porosimetry, respectively. The pore structure is summarized in Table I as pore volumes, separated into three ranges:  $V_{\text{micro}}$ ,  $V_{\text{meso}}$ , and  $V_{\text{macro}}$ . As shown in Table I, the mesopore volume was increased with the PEG/PI ratio, while the micropore volume was kept constant. The size of the mesopore tends to become large with increase of the PEG/PI ratio (Fig. 7). Further, macropores with a size larger than 50 nm were generated in carbonized samples of 4A and 8A (Fig. 8). As a result, the increase of  $V_{\text{meso}}$  was saturated at higher PEG/PI ratios and  $V_{\text{macro}}$  increased instead. The change of the porous structure after carbonization is considered to correlate to the change of the phase-separation structure by the PEG/PI ratio at the polymer stage. In conclusion, the mesopore structure could be con-

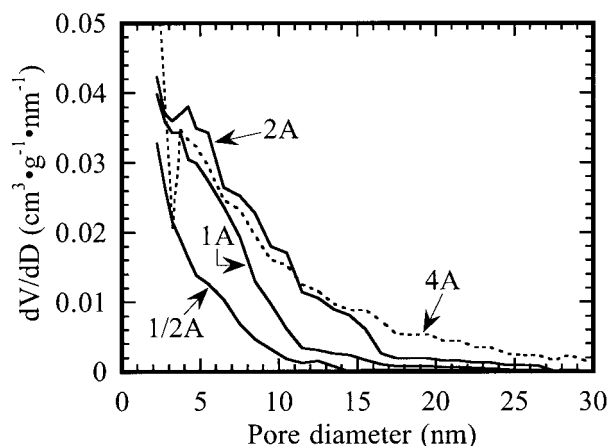


**Figure 7** Pore-size distribution curves determined by nitrogen-adsorption measurement for the samples carbonized at 600°C: 1/2A (PEG2000/PI = 0.43/1), 1A (PEG2000/PI = 0.85/1), 2A (PEG2000/PI = 1.7/1), and 4A (PEG2000/PI = 3.4/1).

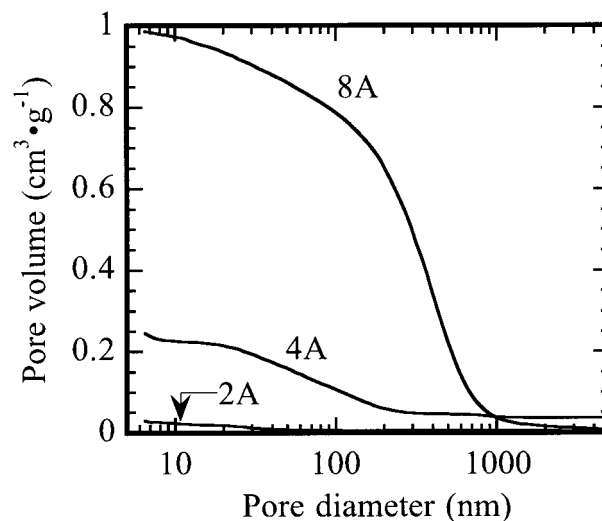


**Figure 8** Cumulative curves of pore volume determined by mercury porosimetry for the samples carbonized at 600°C: 2A (PEG2000/PI = 1.7/1), 4A (PEG2000/PI = 3.4/1), and 8A (PEG2000/PI = 6.8/1).

trolled by the composition of the blended polymers.

The removal of a virus from human plasma was attempted using polymer membranes which have pores with a diameter of 10 or several 10's of nanometers.<sup>21,22</sup> As can be seen from the utilization of carbon material for prostheses, carbon material has the inertness and compatibility for tissue or blood.<sup>23</sup> Application of a mesoporous carbon membrane in the medical field may look promising.

## CONCLUSIONS

Porous carbon films with various pore structures were prepared from a PEG/PI blended polymer. The mesopore-size distribution could be controlled by the composition of these blended polymers, although it was fundamentally independent of the  $M_n$ .

This work was supported by the Japan Society for the Promotion of Science under the RFTF Program No. JSPS-RFTF96R11701.

## REFERENCES

1. Derbyshire, F.; Jagtoyen, M.; Thwaites, M. In *Porosity in Carbon*; Patrick, J. W., Ed., Edward Arnold: London, 1995; Chapter 9.

2. Parkyns, N. D.; Quinn, D. F. In Porosity in Carbon; Patrick, J. W., Ed., Edward Arnold: London, 1995; Chapter 11.
3. Cook, T. L.; Komodromos, C.; Quinn, D. F.; Ragan, S. In Carbon Materials for Advanced Technologies; Burchell, T. D., Ed., Pergamon: Oxford, 1999; Chapter 9.
4. Nishino, A. TANSO 1988, (182), 57–71.
5. Sing, K. S. W.; Everett, D. H.; Haul, R. A. W.; Moscou, L.; Pierotti, R. A.; Rouquerol, J.; Siemieniowska, R. A. Pure Appl Chem 1985, 57, 603–619.
6. Hatori, H.; Yamada, Y.; Shiraishi, M.; Nakata, H.; Yoshitomi, S. Carbon 1992, 30, 305–306.
7. Hatori, H.; Yamada, Y.; Shiraishi, M.; Nakata, H.; Yoshitomi, S.; Yoshihara, M.; Kimura, T. Tanso, 1995, 94–100.
8. Hatori, H.; Yamada, Y.; Shiraishi, M. J Appl Polym Sci 1995, 57, 871–876.
9. Hatori, H.; Yamada, Y.; Shiraishi, M.; Imura, Y.; Kimura, T. Extended Abstracts of 22nd Biennial Conference on Carbon, San Diego, 1995; pp 416–417.
10. Hatori, H.; Doctor Thesis, Hokkaido University, 1996.
11. Pekala, R. W.; Alviso, C. T.; Kong, F. M.; Hulse, S. S. J Non-Cryst Solids 1992, 145, 90–98.
12. Tamai, H.; Kakii, T.; Hirota, Y.; Kumamoto, T.; Yasuda, H. Chem Mater 1996, 8, 454–462.
13. Yoshizawa, N.; Yamada, Y.; Furuta, T.; Shiraishi, M. Energy Fuels 1997, 11, 327–330.
14. Jones, C. W.; Koros, W. Carbon 1994, 32, 1419–1425.
15. Rao, M. B.; Sircar, S. J Membr Sci 1996, 110, 109–118.
16. Petersen, J.; Matsuda, M.; Haraya, K. J Membr Sci 1997, 131, 85–94.
17. Hayashi, J.; Mizuta, H.; Yamamoto, Y.; Kusakabe, K.; Morooka, S. J Membr Sci 1997, 124, 243–251.
18. Dine-Hart, R. A.; Wright, W. W. J Appl Polym Sci 1967, 11, 609–627.
19. Cranston, R. W.; Inkley, F. A. Adv Catal 1957, 9, 143–154.
20. Gregg, S. J.; Sing, K. S. W. In Adsorption, Surface Area and Porosity, 2nd ed.; Academic Press: London, 1991.
21. Tsurumi, T.; Osawa, N.; Hitaka, H.; Hirasaki, T.; Yamaguchi, K.; Manabe, S.; Yamashiki, T. Polym J 1990, 22, 751–758.
22. Sekiguchi, S.; Ito, K.; Kobayashi, M.; Ikeda, H.; Tsurumi, T.; Ishikawa, G.; Manabe, S.; Satani, M.; Yamashiki, T. Membrane 1989, 14, 253–261.
23. Bokros, J.; LaGrange, L. D.; Schoen, F. J. In Chemistry and Physics of Carbon; Walker, P. L., Jr.; Thrower, P. A., Eds.; Marcel Dekker: New York, 1973, pp 103–171.